SCIENCE CHINA
Information Sciences

• RESEARCH PAPER •
Special Focus on 5G Wireless Communication Networks

February 2016, Vol. 59 022303:1–022303:15
doi: 10.1007/s11432-015-5512-6

Channel capacity investigation of a linear massive MIMO system using spherical wave model in LOS scenarios

Liu LIU[1,2,3]*, David W. MATOLAK[2], Cheng TAO[1,3], Yongzhi LI[1], Bo AI[1] & Houjin CHEN[1]

[1]*Institute of Broadband Wireless Mobile Communications, Beijing Jiaotong University, Beijing* 100044*, China;*
[2]*Department of Electrical Engineering University of South Carolina, Columbia, SC* 29208*, USA;*
[3]*National Mobile Communications Research Laboratory, Southeast University, Nanjing* 210096*, China*

Received August 14, 2015; accepted November 24, 2015; published online January 4, 2016

Abstract Massive multiple-input multiple-output (MIMO) is a key technology for the 5th generation (5G) of wireless communication systems. The traditional plane wave channel model (PWM) is often not suitable for the large antenna structure, and in certain cases should be replaced by the more accurate spherical wave model (SWM). By using the spherical wave characterization method, this paper investigates the channel capacity performance of a linear massive MIMO system in line-of-sight (LOS) scenarios. Two types of access settings, the point to point (PTP) system and multi-user (MU) system, are considered. In the PTP setting, a geometrical optimization is performed to obtain configurations that are able to generate a full rank channel matrix for a linear massive MIMO system, which yields full spatial diversity even in LOS scenarios. Compared with the approximate and commonly applied rank-1 PWM, this is very useful for fixed wireless access and radio relay systems requiring high throughput. For the MU case, we compare the eigenvalue distributions of the LOS channels using the plane wave and spherical wave characterization method, and sum rate results are obtained by Monte Carlo simulations. The results show that MU systems using the more realistic and accurate SWM can achieve a higher sum rate than results from the PWM. This is beneficial and informative when designing massive MIMO wireless networks.

Keywords massive MIMO, channel model, plane wave model, spherical wave model, channel capacity

Citation Liu L, Matolak D W, Tao C, et al. Channel capacity investigation of a linear massive MIMO system using spherical wave model in LOS scenarios. Sci China Inf Sci, 2016, 59(2): 022303, doi: 10.1007/s11432-015-5512-6

1 Introduction

Massive multiple-input multiple-output (MIMO) is an emerging technology that is a prime candidate for use in the 5th generation (5G) of wireless communication systems. Massive MIMO systems can provide high data throughput, communication reliability, and high power efficiency with relatively simple signal processing [1–4]. In a massive MIMO cellular system, the base-station is equipped with a large number of (e.g., more than 100) antenna elements, and simultaneously serves many tens of terminals

* Corresponding author (email: liuliu@bjtu.edu.cn)

in the same-frequency resource. These terminals have few (sometimes one, or likely no more than two) antennas.

In the conventional channel propagation characterization, the propagation "rays" are assumed to be perpendicular to the constant-phase planes, and these rays are approximately parallel. This is the traditional plane wave model (PWM). In the plane wave assumption, the wave arriving at the array can be represented by a simple plane wave with constant amplitude across the array, and thus the directions of the plane wave arrivals are considered the same. This model is appropriate for the compact antenna structure. When the antenna span is large (e.g., 6.35 m if 128 antenna elements are used at 3 GHz), this assumption is no longer suitable. Accordingly, a spherical wave model should be employed for massive MIMO channel characterizations [5,6].

On the other hand, the advantages of massive MIMO systems lie in the key assumption that the channel vector (e.g., a channel vector is $\boldsymbol{h}_i = [h_{i,1}, h_{i,2}, \ldots, h_{i,M}]^{\mathrm{T}}$, where $h_{i,m}$ $(1 \leqslant m \leqslant M)$ is the complex channel gain from the receiver antenna element i to the transmitter antenna element m, and M is the number of elements at the transmitter) should be pairwise orthogonal, and here we term this the favorable propagation condition [1,7]. By using the law of large numbers, this strict condition can be approximately achieved when entries of the channel vector are independent and identically distributed (i.i.d.) Gaussian complex variables [1,3,7,8]. This asymptotically favorable propagation condition is the one of the key requirements to ensure that linear signal processing can achieve the optimal performance. Under this condition, the matched filter achieves the nearly optimal performance at the base-station. The multiuser interference and the thermal noise can be substantially suppressed. However, in realistic propagation environments, this favorable channel conditions are not always met, e.g., in line-of-sight (LOS) environments. In the LOS scenario, when the plane wave model is used, the channel vectors are highly correlated. Hence, the rank of the channel matrix will be one. The benefit of the very tall or very wide matrix in large MIMO system would not be achieved any more [1].

In massive MIMO systems, a special condition is that the distance between the transmitter and receiver may be less than the Rayleigh distance due to the huge size of the antenna structure. The Rayleigh distance is a common criterion for defining the boundary between the far field and near field. Within the near field, the phase and the amplitude will change significantly across the array. This issue is obvious for a linear massive MIMO system because of its large antenna array size and one-dimensional shape. The channel fading coefficients observed from different elements will change remarkably when the transmission distance is less than the Rayleigh distance. Even in LOS propagation environments, without multipath components, the channel matrix could also be made high rank by using the more realistic spherical wave compared with the plane wave. This interesting result is similar to that provided in [9–11].

The Mobile and wireless communications Enablers for the Twenty-twenty Information Society (METIS) project has laid out 12 application cases for future mobile and wireless systems [12]. Some of these cases are categorized as LOS scenarios, such as a stadium and a shopping hall. As noted, the millimeter wave frequency band may be employed for the 5G wireless communication system [13]. This means that substantial portion of propagation conditions will be short range (small cells [14]) and with LOS present, in order to avoid the large path loss introduced by distance and NLOS conditions. In this paper, we investigate the channel capacity and sum rate performance of the point to point (PTP) and multi-user (MU) linear massive MIMO systems in LOS propagation environments by using a geometrical channel characterization method. In [1], it was presented that the performance of a massive MIMO system is disappointing in LOS propagation. The performance results are based on the assumption of plane wave propagation, but if the realistic and accurate spherical wave model (SWM) is employed, the results change significantly. The main contributions of this paper are as follows:

• By using the theoretical SWM, we propose an optimization method by which the orthogonality condition of the PTP system can be achieved via the geometrical ray tracing method. This method specifies some explicit values for the transmitter and receiver distance, the element separation and the rotation angle of the antenna array. It can make the vectors of the channel matrix orthogonal, and make the matrix have a large rank. Under this condition, almost full channel capacity can be obtained even in LOS environments. It is different from the conventional optimization method used in small MIMO

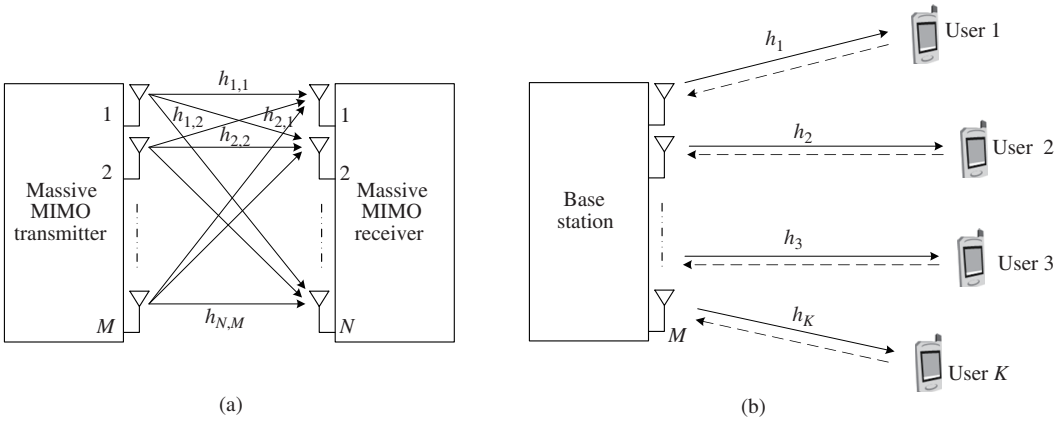

Figure 1 Block diagram of the PTP system and MU system. (a) PTP structure; (b) MU structure.

system. Such a condition can be easily ensured in the massive MIMO fixed wireless access relay systems under LOS conditions for capacity improvement. In particular, a millimeter wave signal is preferred for this optimization method to ensure a small and compact antenna structure.

• By using the SWM method, the sum rate capacity results of the MU massive MIMO are investigated and the results are verified by the Monte Carlo simulation method. The results reveal that the user terminals served by the massive MIMO base-station also can obtain the spatial diversity gain even in LOS scenarios. In particular, the sum rate results obtained from the SWM are higher than those from the PWM, and more closely approach those attainable results in the favorable propagation condition.

The rest of the paper is organized as follows. Section 2 reviews the channel descriptions and backgrounds. In Section 3 we use the plane wave and spherical wave model to characterize the PTP linear massive MIMO propagation channel, and derive the orthogonality condition which can make the matrix have a large rank. In Section 4 we model the MU linear massive MIMO channels using the plane wave and spherical wave methods, and then compare the eigenvalue distributions of these two types of models. The simulation results using the ray-tracing method are present in Section 5, and conclusions are drawn in Section 6.

2 System model

The block diagram of the PTP and MU linear massive MIMO systems is shown in Figure 1. We assume that the antenna elements at both link ends are perfectly omnidirectional. We also assume that the transmitter and receiver separation distance is much larger than the Rayleigh distance of a single element. We consider only pure LOS rays in the propagation environment, i.e., there are no multipath components in this benign environment.

In a massive MIMO system, both the transmitter and receiver can be provided with a large number of antennas. The transmitter is equipped with M antenna elements, and the receiver antenna has an array of N antenna elements. Assuming a time invariant channel, we characterize the complex narrowband channel matrix $\boldsymbol{H}_{N\times M}$. We normalize the power of the channel coefficients to unity, i.e., all the elements in $\boldsymbol{H}$ have constant amplitude of one on the average. Hence, $\boldsymbol{H}$ is a small scale fading channel matrix. We now define an important matrix which will be used in the capacity calculation as

$$\boldsymbol{W} = \begin{cases} \boldsymbol{H}\boldsymbol{H}^{\mathrm{H}}, & M > N, \\ \boldsymbol{H}^{\mathrm{H}}\boldsymbol{H}, & M \leqslant N, \end{cases} \tag{1}$$

where $(\cdot)^{\mathrm{H}}$ denotes the Hermitian transpose operation. Let $\{\mu_i\}_{i=1}^{\min\{M,N\}}$ be the eigenvalues of $\boldsymbol{W}$ in ascending order. The number of non-zero eigenvalues μ_i is equal to the rank of $\boldsymbol{W}$, and it is also equal to the number of degrees of freedom of the channel matrix $\boldsymbol{H}$ which quantifies the achievable diversity gain. In our analysis, we use the fact that $\{\mu_i\}$ is subject to the constraint $\sum \mu_i = \mathrm{trace}(\boldsymbol{W}) = MN$ [15]. We

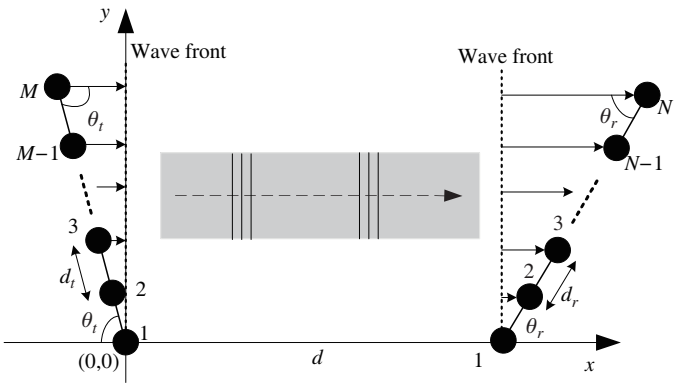

Figure 2 General massive MIMO plane wave model.

denote by $\tilde{\mu}$ the largest eigenvalue which corresponds to $\tilde{\mu} = MN$ when $\boldsymbol{W}$ has rank one. Additionally, we denote $\min\{M, N\} = U$ and $\max\{M, N\} = V$. From basic knowledge of the channel capacity [16], it is known that each non-zero eigenchannel (each μ_i corresponds to an eigenmode of the channel) can support a data stream; thus, if $\mu_1 = \mu_2 = \cdots = \mu_U$, the maximum channel capacity can be achieved.

We assume that an average transmit power over the array is equally allocated, thus the channel capacity of a MIMO system ($M > N$) is described as

$$C = \log_2 \det\left(\mathbf{I}_N + \frac{\rho}{M}\boldsymbol{W}\right), \tag{2}$$

where $\mathbf{I}_N$ is the N by N identity matrix, and ρ is the per-channel signal to noise ratio (SNR). The channel capacity can be calculated by using the eigenvalue as

$$C = \log_2 \det\left(\mathbf{I}_N + \frac{\rho}{M}\boldsymbol{W}\right) = \sum_{i=1}^{\min(M,N)} \log_2\left(1 + \frac{\rho \cdot \mu_i}{M}\right). \tag{3}$$

When a PTP massive MIMO system is separated at one end, a MU system can be obtained. It is assumed that the transmitter (base-station side) has M transmit antennas and K users (each user is equipped with a single receive antenna) are served simultaneously. The users do not collaborate, neither transmitting data nor the channel information. In [1,3], the channel of the MU system is characterized by multiplying two matrices $\boldsymbol{D}$ and $\boldsymbol{H}$, where $\boldsymbol{D}$ accounts for the large scale fading and $\boldsymbol{H}$ accounts for the small scale fading. In this paper, we only focus on the small scale fading properties of the spherical wave model. We can assume that the large scale fading matrix $\boldsymbol{D}$ is represented by an identity matrix for simplicity [3].

3 Plane wave vs. spherical wave model for PTP MIMO capacity

3.1 PTP channel capacity using plane wave model

Figure 2 provides the illustration of the plane wave model for a PTP massive MIMO system. For the PTP massive MIMO system, a plane wave from the transmitter array arrives at the receiver antenna array, and d is the distance between the 1st transmitter antenna element and the 1st receiver antenna element. θ_t and θ_r are the orientation angles of the transmitter array and receiver array with respect to the x axis. d_t and d_r are the element separations of the transmitter and receiver antenna array. Then the path length differences among elements only depend on the additional path lengths from $d_t \cos\theta_t$ and $d_r \cos\theta_r$, but not on the realistic propagation ray. Based on the plane wave model, the PTP massive MIMO channel matrix $\boldsymbol{H}_{N\times M}^{\mathrm{PP}}$ is given by [17]

$$\boldsymbol{H}_{N\times M}^{\mathrm{PP}} = \psi \boldsymbol{\alpha}_R \boldsymbol{\alpha}_T^{\mathrm{H}}, \tag{4}$$

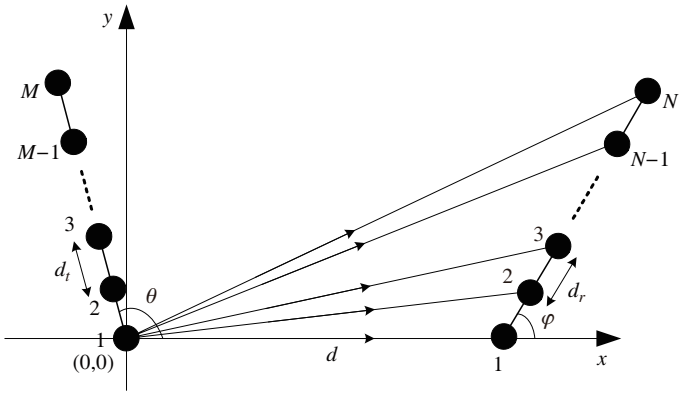

Figure 3 General channel characterization of massive MIMO using the SWM.

where the spatial signature vectors are given as

$$\boldsymbol{\alpha}_R = \left[1, \exp\left(\mathrm{j}\frac{2\pi}{\lambda} d_r \cos\theta_r\right), \ldots, \exp\left(\mathrm{j}\frac{2\pi}{\lambda}\left(N-1\right) d_r \cos\theta_r\right)\right]^{\mathrm{T}}, \tag{5}$$

$$\boldsymbol{\alpha}_T = \left[1, \exp\left(\mathrm{j}\frac{2\pi}{\lambda} d_t \cos\theta_t\right), \ldots, \exp\left(\mathrm{j}\frac{2\pi}{\lambda}\left(M-1\right) d_t \cos\theta_t\right)\right]^{\mathrm{T}}, \tag{6}$$

and

$$\psi = \exp\left(\mathrm{j}\frac{2\pi}{\lambda} d\right). \tag{7}$$

The first superscript P of $\boldsymbol{H}_{N\times M}^{\mathrm{PP}}$ represents the PTP structure, and the second P represents the plane wave model. $(\cdot)^{\mathrm{T}}$ is the vector transpose operator.

According to matrix theory, we can obtain $\mathrm{rank}(\boldsymbol{H}_{N\times M}^{\mathrm{PP}}) = \mathrm{rank}(\boldsymbol{W}^{\mathrm{PP}}) = 1$ because all columns/rows of $\boldsymbol{H}_{N\times M}^{\mathrm{PP}}$ are linearly dependent. This means that $\mathrm{rank}(\boldsymbol{H}_{N\times M}^{\mathrm{PP}})$ is independent of the geometrical parameters, the separation distance d, and orientation angles θ_t and θ_r. Then the unique non-zero eigenvalue $\tilde{\mu}$ of the matrix $\boldsymbol{W}^{\mathrm{PP}}$ satisfies $\tilde{\mu} = MN$, hence by using the relationship between the channel capacity and the eigenvalue (1)–(3), the PTP channel capacity expressions using the PWM are

$$C_{M>N}^{\mathrm{PP}} = \log_2 \det\left(\boldsymbol{I}_N + \frac{\rho}{M}\left(\boldsymbol{H}_{N\times M}^{\mathrm{PP}}\right)\left(\boldsymbol{H}_{N\times M}^{\mathrm{PP}}\right)^{\mathrm{H}}\right) = \log_2\left(1+\rho N\right) = \log_2\left(1+\rho U\right), \tag{8}$$

and

$$C_{M\leqslant N}^{\mathrm{PP}} = \log_2 \det\left(\boldsymbol{I}_M + \frac{\rho}{N}\left(\boldsymbol{H}_{N\times M}^{\mathrm{PP}}\right)^{\mathrm{H}}\left(\boldsymbol{H}_{N\times M}^{\mathrm{PP}}\right)\right) = \log_2\left(1+\rho M\right) = \log_2\left(1+\rho U\right). \tag{9}$$

It can be seen from (8) and (9), for the LOS plane wave model, the addition of more antennas can only boost the effective SNR. It yields a logarithmic increase in capacity in massive MIMO channels. No spatial diversity can be achieved, and only the gain for the SNR enhancement can be obtained.

3.2 PTP channel capacity using spherical wave model

A spherical wave model characterizes the channel using a geometrically accurate method in the propagation environment. We assume that the 1st element of the transmitter antenna is located at the coordinate origin. The propagation environment is shown in Figure 3.

We use the vectors to describe the coordinates of the transmitter antenna element and receiver antenna element, which are given as

$$\boldsymbol{r}_m^{\mathrm{PST}} = \left(m-1\right) d_t \cos\theta\ \boldsymbol{x} + \left(m-1\right) d_t \sin\theta\ \boldsymbol{y}, \tag{10}$$

and

$$\boldsymbol{r}_n^{\mathrm{PSR}} = \left(d + \left(n-1\right) d_r \cos\varphi\right)\ \boldsymbol{x} + \left(n-1\right) d_r \sin\varphi\ \boldsymbol{y}, \tag{11}$$

where $\boldsymbol{x}$ and $\boldsymbol{y}$ represent the unit vector in their respective x and y directions. The superscript PST and PSR represent the PTP spherical wave at the transmitter and receiver, respectively. Then the propagation path length (direct line) between the mth transmitter element of the transmitter array and nth receiver element of the receiver array is

$$\begin{aligned} r_{n,m}^{\mathrm{PS}} &= \left\| \boldsymbol{r}_m^{\mathrm{PST}} - \boldsymbol{r}_n^{\mathrm{PSR}} \right\| \\ &= \left\{ \left[d + (n-1)\, d_r \cos\varphi - (m-1)\, d_t \cos\theta \right]^2 + \left[(n-1)\, d_r \sin\varphi - (m-1)\, d_t \sin\theta \right]^2 \right\}^{1/2}. \end{aligned} \tag{12}$$

Then the matrix $\boldsymbol{H}_{N\times M}^{\mathrm{PS}}$ is given as

$$\boldsymbol{H}_{N\times M}^{\mathrm{PS}} = \left[\boldsymbol{h}_1^{\mathrm{PS}}, \boldsymbol{h}_2^{\mathrm{PS}}, \ldots, \boldsymbol{h}_N^{\mathrm{PS}} \right]^{\mathrm{T}}, \tag{13}$$

where the row vector $\boldsymbol{h}_n^{\mathrm{PS}}$ is expressed as

$$\boldsymbol{h}_n^{\mathrm{PS}} = \left[\exp\left(\mathrm{j}\frac{2\pi}{\lambda} r_{n,1}^{\mathrm{PS}} \right), \exp\left(\mathrm{j}\frac{2\pi}{\lambda} r_{n,2}^{\mathrm{PS}} \right), \ldots, \exp\left(\mathrm{j}\frac{2\pi}{\lambda} r_{n,M}^{\mathrm{PS}} \right) \right]. \tag{14}$$

Note that the first superscript character P represents the PTP structure, and S represents the spherical wave model.

When $M > N$, $\boldsymbol{W}_{N\times N}^{\mathrm{PS}} = \boldsymbol{H}_{N\times M}^{\mathrm{PS}} \left(\boldsymbol{H}_{N\times M}^{\mathrm{PS}} \right)^{\mathrm{H}}$ with the element of the inner product of $\boldsymbol{H}_{N\times M}^{\mathrm{PS}}$ is given as

$$\left(\boldsymbol{W}_{N\times N}^{\mathrm{PS}} \right)_{n_1,n_2} = \left\langle \boldsymbol{h}_{n_1}^{\mathrm{PS}}, \left(\boldsymbol{h}_{n_2}^{\mathrm{PS}} \right)^{\mathrm{H}} \right\rangle = \sum_{m=1}^{M} \exp\left(\mathrm{j}\frac{2\pi}{\lambda} \left(r_{n_1,m}^{\mathrm{PS}} - r_{n_2,m}^{\mathrm{PS}} \right) \right). \tag{15}$$

According to the matrix theory, we know that the orthogonality between the different vectors can be obtained only when

$$\left(\boldsymbol{W}_{N\times N}^{\mathrm{PS}} \right)_{n_1,n_2} = \sum_{m=1}^{M} \exp\left(\mathrm{j}\frac{2\pi}{\lambda} \left(r_{n_1,m}^{\mathrm{PS}} - r_{n_2,m}^{\mathrm{PS}} \right) \right) = \begin{cases} M, & \text{if } n_1 = n_2, \\ 0, & \text{if } n_1 \neq n_2. \end{cases} \tag{16}$$

From (16), we can see that if we can select suitable values of the transmitter and receiver distance, the element separation and the rotation angle of the antenna array, the orthogonality could be met. After some practical approximations (the detailed derivation of which is given in Appendix), if the transmitter antenna array and receiver antenna array are parallel ($\theta = \varphi = \pi/2$), two orthogonality conditions are given as

$$d = \frac{d_a^2 V}{\lambda Z} \tag{17}$$

and

$$d_a > Z \cdot 10\lambda, \tag{18}$$

where Z is a positive nonzero integer, and here we assume that the element separation of the transmitter and receiver antenna is the same, denoted as $d_t = d_r = d_a$. Simulation results are provided in Section 5 for verification of (17) and (18). Compared with the rank-1 channel matrix from the PWM, the PTP massive MIMO channel matrix can achieve full rank which can increase the channel capacity substantially. Some remarks are in order:

1. According to (17), there are several distance choices for the orthogonal transmission configuration if Z equals different integer values. The basic criterion depends on the path loss, and the limitation of the antenna structure and size.

2. Eq. (18) goes beyond the traditional element separation value $d_a = \lambda/2$. It is also in line with the fact that an expansion in space domain will bring benefits. When this criterion is put into practice, a millimeter wave signal is preferred. This is because the relatively large value of V does not yield a huge antenna physical span when the millimeter wave signal is used.

3. If the geometrical requirements are satisfied according to the wavelength λ, the wireless communication system achieving almost full diversity can work at different frequency bands, regardless of Ultra High Frequency (HUF) or Super High Frequency (SHF).

4. The increased element separation can also alleviate the coupling effect of neighboring antennas. This is beneficial to the physical antenna design and optimization.

4 Plane wave vs. spherical wave model for MU MIMO sum rate

4.1 MU MIMO sum rate using plane wave model

In MU massive MIMO systems, antenna arrays with a few hundred antennas, simultaneously serve many tens of terminals in the same time-frequency resource [2]. We so assume that $M > K$. Figure 4 illustrates the propagation principle of a MU massive MIMO system using the plane wave. The propagation channel coefficient only depends on the propagation distance between the antenna array and the user k, and the plane wave generated incidence angle of θ_k.

Due to the plane wave assumption, the propagation paths from each antenna element to the user k are parallel and simplified as R_k. Then the channel coefficient matrix of the uplink is given as

$$\boldsymbol{H}_{M\times K}^{\mathrm{MP}} = \left[\boldsymbol{h}_1^{\mathrm{MP}}, \boldsymbol{h}_2^{\mathrm{MP}}, \ldots, \boldsymbol{h}_K^{\mathrm{MP}}\right], \tag{19}$$

where the kth column channel vector is given as

$$\boldsymbol{h}_k^{\mathrm{MP}} = \exp\left(\mathrm{j}\frac{2\pi}{\lambda}R_k\right)\left[1, \exp\left(-\mathrm{j}\frac{2\pi}{\lambda}d_t\sin\theta_k\right), \ldots, \exp\left(-\mathrm{j}\frac{2\pi}{\lambda}\left(M-1\right)d_t\sin\theta_k\right)\right]^{\mathrm{T}}. \tag{20}$$

In (19) and (20), the first superscript M denotes the MU structure, and P represents the plane wave model. It can be found that the signals received/transmitted at adjacent antenna elements differ in phase by $2\pi d_t\sin\theta_k/\lambda$ due to the relative delay. In the same manner, $\boldsymbol{W}^{\mathrm{MP}} = (\boldsymbol{H}_{M\times K}^{\mathrm{MP}})^{\mathrm{H}}\boldsymbol{H}_{M\times K}^{\mathrm{MP}}$ whose element is the inner product of the column channel in $\boldsymbol{H}_{M\times K}^{\mathrm{MP}}$ is (assuming that two users are not at the exact same spatial location)

$$\begin{aligned}\left(\boldsymbol{W}^{\mathrm{MP}}\right)_{k_1,k_2} &= \left\langle\left(\boldsymbol{h}_{k_1}^{\mathrm{MP}}\right)^{\mathrm{H}}, \boldsymbol{h}_{k_2}^{\mathrm{MP}}\right\rangle = \sum_{m=1}^{M}\exp\left(\mathrm{j}\frac{2\pi}{\lambda}d_t\left(\sin\theta_{k_1}-\sin\theta_{k_2}\right)\left(m-1\right)\right)\\ &= \frac{\sin(\frac{\pi}{\lambda}d_t(\sin\theta_{k_1}-\sin\theta_{k_2})M)}{\sin(\frac{\pi}{\lambda}d_t(\sin\theta_{k_1}-\sin\theta_{k_2}))}.\end{aligned} \tag{21}$$

Similar to the previous results, it can be shown that the matrix becomes a diagonal one if the inner product of $(\boldsymbol{h}_{k_1}^{\mathrm{MP}})^{\mathrm{H}}$ and $\boldsymbol{h}_{k_2}^{\mathrm{MP}}$ is equal to zero. So we have

$$\left|\frac{1}{\lambda}d_t\left(\sin\theta_{k_2}-\sin\theta_{k_1}\right)M\right| = Z_1, \tag{22}$$

where Z_1 is a nonzero integer. Note that the general solution of (21) is independent of the separation distance R_k. However, since the users in a cell are nomadic, it makes no sense to characterize the differences of fixed orientation angles and separation distances. For the MU setting, statistical results using the Monte Carlo simulation method are presented subsequently.

4.2 MU MIMO sum rate using spherical wave model

In the SWM, the channel coefficient is directly obtained from the actual path ray between the user k and each antenna element, as shown in Figure 5. Similar to the previous method, the vectors locating the user k and antenna element m are given as

$$\boldsymbol{r}_k^u = R_k\cos\theta_k\boldsymbol{x} + R_k\sin\theta_k\boldsymbol{y} \tag{23}$$

and

$$\boldsymbol{r}_m^A = dt\left(m-1\right)\boldsymbol{y}, \tag{24}$$

respectively. Then the propagation path length between the user k and mth transmitter element is

$$r_{k,m}^{\mathrm{MS}} = \left\|\boldsymbol{r}_k^u - \boldsymbol{r}_m^A\right\| = \left[\left(R_k\cos\theta_k\right)^2 + \left(R_k\sin\theta_k - dt\left(m-1\right)\right)^2\right]^{1/2}, \tag{25}$$

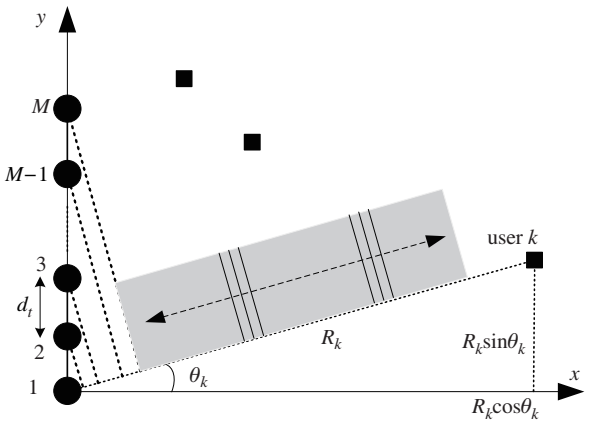

Figure 4 Principle of the MU massive MIMO channel using the PWM.

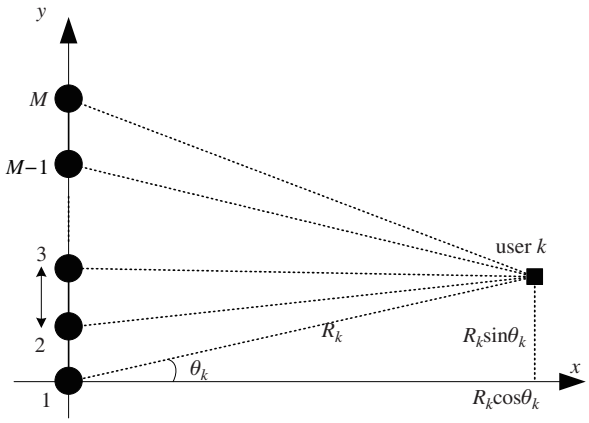

Figure 5 Principle of the MU massive MIMO channel using the SWM.

where the first superscript character M represents the MU structure, and the letter S represents the spherical wave model. Similarly, the channel coefficient matrix of the uplink is given as

$$\boldsymbol{H}_{M\times K}^{\mathrm{MS}} = \left[\boldsymbol{h}_1^{\mathrm{MS}}, \boldsymbol{h}_2^{\mathrm{MS}}, \ldots, \boldsymbol{h}_K^{\mathrm{MS}}\right], \tag{26}$$

where the kth column channel vector is given as

$$\boldsymbol{h}_k^{\mathrm{MS}} = \left[\exp\left(\mathrm{j}\frac{2\pi}{\lambda}r_{k,1}^{\mathrm{MS}}\right), \exp\left(\mathrm{j}\frac{2\pi}{\lambda}r_{k,2}^{\mathrm{MS}}\right), \ldots, \exp\left(\mathrm{j}\frac{2\pi}{\lambda}r_{k,M}^{\mathrm{MS}}\right)\right]^{\mathrm{T}}. \tag{27}$$

Then $\boldsymbol{W}^{\mathrm{MS}} = \left(\boldsymbol{H}_{M\times K}^{\mathrm{MS}}\right)^{\mathrm{H}} \boldsymbol{H}_{M\times K}^{\mathrm{MS}}$ is

$$\left(\boldsymbol{W}^{\mathrm{MS}}\right)_{k_1,k_2} = \left\langle \left(\boldsymbol{h}_{k_2}^{\mathrm{MS}}\right)^{\mathrm{H}}, \boldsymbol{h}_{k_1}^{\mathrm{MS}} \right\rangle = \sum_{m=1}^{M} \exp\left(\mathrm{j}\frac{2\pi}{\lambda}\left(r_{k_1,m}^{\mathrm{MS}} - r_{k_2,m}^{\mathrm{MS}}\right)\right). \tag{28}$$

According to (28), it is impossible to derive a closed-form solution for the orthogonality condition since in the MU massive MIMO scenario, different users have their own different and completely arbitrary values of transmission distance and orientation angles with respect to the antenna array. Here, the statistic simulation method is a good resort.

In theory, sum rate results depend on the eigenvalue distributions of the channel matrix. Generally, the less spread out the eigenvalues, or equal eigenvalues in the limiting case, the larger achievable capacity. In this paper, we use the ray tracing simulation method to compare the eigenvalue distributions of channel matrices characterized by the PWM and SWM. Ray tracing is based on finding the path length from each of the transmitter antennas to each of the receiver antennas, and employing these path lengths to find the corresponding received phases. We consider the simulation case in which the base-station having M antenna elements serves K independently distributed users in a certain wireless range. The base-station is located in the center of the range. We employ the mean square error (MSE) to evaluate the difference among the two eigenvalue distributions. The MSE is given as

$$\mathrm{MSE} = \frac{1}{I}\sum_{i=1}^{I}\left(p_i^S - p_i^P\right)^2, \tag{29}$$

where p_i^S and p_i^P are the eigenvalue distribution values at the ith possible value, and I is the length of the eigenvalue distribution. Here we use the distribution spread width corresponding to 95th percentile. Table 1 lists the MSE results for the eigenvalue distribution difference between different antenna configurations at values of the cell radius R_c. In the conventional definition of the far region boundary, it is defined in the radially outward direction. In [18], the far field is defined as the area in which the

Table 1 Eigenvalue distribution MSE results of the PWM and the SWM[a)]

$\leqslant 0.95$	$M = 64,\ R_{\mathrm{FRBLMA}} = 794$ m			$M = 128,\ R_{\mathrm{FRBLMA}} = 3226$ m			
K	8	16	32	8	16	32	64
$R_c \leqslant R_{\mathrm{FRBLMA}}/40$	0.066	0.048	0.024	0.077	0.059	0.047	0.026
$R_c \leqslant R_{\mathrm{FRBLMA}}/4$	0.012	0.015	0.019	0.012	0.013	0.017	0.022
$R_c \leqslant R_{\mathrm{FRBLMA}}/2$	0.011	0.014	0.020	0.011	0.012	0.016	0.021
$R_c \leqslant R_{\mathrm{FRBLMA}}$	0.009	0.013	0.021	0.010	0.011	0.015	0.022
$R_c \leqslant 2R_{\mathrm{FRBLMA}}$	0.008	0.012	0.022	0.009	0.010	0.014	0.022

a) $R_c \leqslant R_{\mathrm{FRBLMA}}/40$ is a limitation example for comparison which is not connected to any practical criterion. MSE values in $R_c \leqslant R_{\mathrm{FRBLMA}}/40$ can be considered as the upper bound of the difference gap of the two models.

minimum pure spherical wave caused phase difference is less than $\pi/8$ (22.5°). Using this criterion, we have derived that when $d_t = \lambda/2$, the Far Region Boundary of Linear Massive Antenna (FRBLMA) is $R_{\mathrm{FRBLMA}} = 2\left(M-1\right)^2\lambda$ [19]. We also assume that users are randomly distributed in the cell coverage area. All these are provided in Table 1. The central frequency f_c is assumed to be 3 GHz corresponding to the wavelength $\lambda = 0.1$ m. The element separation at the base-station is $\lambda/2$. Note that

1. In future wireless communication networks, the small cell configuration is a main trend especially for high capacity reasons. Most of the time, the radius of a cell is several hundred meters [14,20].

2. As for the number of users in each cell, it is noted in [1,2] that the antenna array at the base-station equipped with a few hundred antennas serves many tens of users which can generate very tall or very wide channel matrices. Tall or wide matrices tend to be very well conditioned. For this reason, we consider the cases in which $K/M \leqslant 0.5$.

Table 1 provides the eigenvalue distribution deviation caused by different values of the ratio K/M. As shown in this table, MSE results are at a low level on the average. In particular, MSE values decrease as the wireless coverage R_c increases (except for $R_c \leqslant R_{\mathrm{FRBLMA}}/40$). This is because when the wireless range increases, the distance between the randomly distributed user and the base-station can become large (increasing users distribute in the far field region), and the arrival angle difference values of each propagation ray tend to be relatively small: the spherical wave tends to the plane wave. For any ranges, except $R_c \leqslant R_{\mathrm{FRBLMA}}/40$, MSE values increase with the number of users K. This is due to the reason that when K/M increases, the PWM generated channel matrix $\boldsymbol{W}^{\mathrm{MP}}$ is more likely to be ill-conditioned than the SWM generated channel matrix $\boldsymbol{W}^{\mathrm{MS}}$. The SWM generated channel matrix contains much more diverse path length and angle variations.

5 Simulation results

5.1 Plane wave vs. spherical wave for PTP massive MIMO systems

The PTP massive MIMO system can be used for backhaul transmission, e.g., MIMO fixed wireless access relay systems. In practical applications, the working frequency band, the number of antenna elements, antenna element separation, distance between the transmitter antenna and receiver antenna and the orientation angle are the main factors the system designers may jointly optimize. Here, we use the ray tracing simulation method to verify the orthogonality conditions provided as (17) and (18). Considering $d_a > 10\lambda$, we use $d_a = 12\lambda$. The millimeter wave band with the central frequency of 30 GHz is chosen to ensure a small and compact antenna structure. For clear understanding and comparison of the practical system, we also provide the parameters for the system working at 60 GHz. It has been stated that if two orthogonality conditions are satisfied, the wireless communication system can work at different frequency bands. In the simulation settings, we assume that the transmitter antenna array is equipped with 128 antenna elements, and the receiver has 8, 16, 32 and 64 antenna elements. It can be seen from (17) and (18) that the eigenvalue distributions are independent of the working frequency. Table 2 describes the simulation physical parameters.

Table 2 Physical parameters of the PTP massive MIMO system

$Z = 1$	Antenna span ($d_a = 12\lambda$) (m)				$d = d_a^2 V/Z\lambda$ (m)
Element number $N = U$	8	16	32	64	$M = V = 128$
30 GHz, $\lambda = 0.01$ m	0.84	1.80	3.72	7.56	184
60 GHz, $\lambda = 0.005$ m	0.42	0.90	1.86	3.78	92

Due to the significant path loss when using the millimeter wave signals, short range transmission is most suitable. We consider range values less than 500 m.

Figure 6 provides the eigenvalues of the PTP massive MIMO system for both the orthogonal configuration and the plane wave assumptions. The results are obtained at the central frequency at 30 GHz, and the results of 60 GHz are identical. The blue lines, corresponding to the left ordinate, are the eigenvalues of $M = 128$ transmitter elements working with $N = 8$, $N = 16$, $N = 32$ and $N = 64$ receiver elements under the orthogonality conditions from the SWM. It is obvious that if the conditions of (17) and (18) are satisfied, all the eigenvalues of the matrix $\boldsymbol{W}$ are distributed around unity. In numerical analysis, $\mu_{\max}/\mu_{\min}$ is defined to be the condition number of the matrix $\boldsymbol{W}$. The matrix is said to be well-conditioned if the condition number is close to 1 [17]. Under this condition, the highest channel capacity can be achieved, and hence the system configuration can provide N spatial degrees of freedom. This finding can be verified in the capacity simulation results in Figure 7, discussed subsequently. In particular, considering all the possible eigenvalue distributions of a simulation case, we can see the deviation of the eigenvalue from the unit value increases as the number of receiver elements increases. This is because very tall or very wide matrices tend to be very well conditioned and hence tend to have equal eigenvalues [1]. On the other hand, the black lines in Figure 6, corresponding to the right ordinate, are the eigenvalues results of the plane wave assumption. The results show that there is only the one non-zero eigenvalue $\tilde{\mu}$ of the matrix $\boldsymbol{W}$, equaling N. This is called the ill-conditioned matrix. Under the ill-conditioned propagation environment, no spatial diversity can be obtained.

Figure 7 gives the channel capacity results of the different simulation cases specified in Table 2. It can be seen that even in LOS scenarios, if the orthogonality conditions are met, channel capacities increase significantly as the number of antenna elements increases when using the more realistic spherical wave model (dotted blue lines). We also present the results when the channels are truly orthogonal (red marks), which are the channel capacity upper bounds (Eq. (9) in [1]). The figure explicitly shows that when using the SWM, the LOS capacity results under the orthogonality conditions and the upper bounds are essentially identical. This means that the full spatial diversity can be obtained in LOS scenarios through appropriate configuration. As for the plane wave results, only an SNR gain from multiple receiver antennas can be obtained due to the rank deficiency of the channel matrix $\boldsymbol{H}$. In addition, the i.i.d. Rayleigh results are provided in Figure 7, from which we can see there is a capacity gap from the spherical wave result when the element number of the receiver antenna is relatively large. This gap shrinks with decreasing the size of the receiver antenna array. This also can be attributed to the well-conditioned property of the tall or wide matrix.

5.2 Plane wave vs. spherical wave for MU massive MIMO systems

In Subsection 4.2, based on the MSE simulation results, it was found that the eigenvalues of the plane wave and spherical wave models appeared approximately in the same distribution in different sized cells. The MSE value is a first-order but crude measure due to the fact that there is a large number of eigenvalues distributed around the zero value, both for the PWM and SWM, yielding a small MSE difference after the averaging operation. However, the nonzero eigenvalues actually do contribute to the sum rate of the transmission system. Thus the final sum-rate results of the linear massive MIMO system using the plane wave model and spherical model are considered in this section. One way of quantifying the difference among the channel responses of different terminals, is to look at the eigenvalue spread of eigenvalues of the matrix $\boldsymbol{W}$.

Figure 8 illustrates this for a case with different numbers of users and a base-station having 64 and

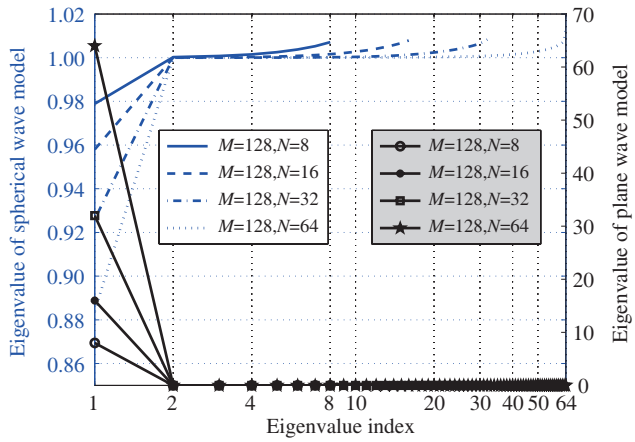

Figure 6 Comparison results of eigenvalue distributions of the plane wave model and the orthogonal configuration.

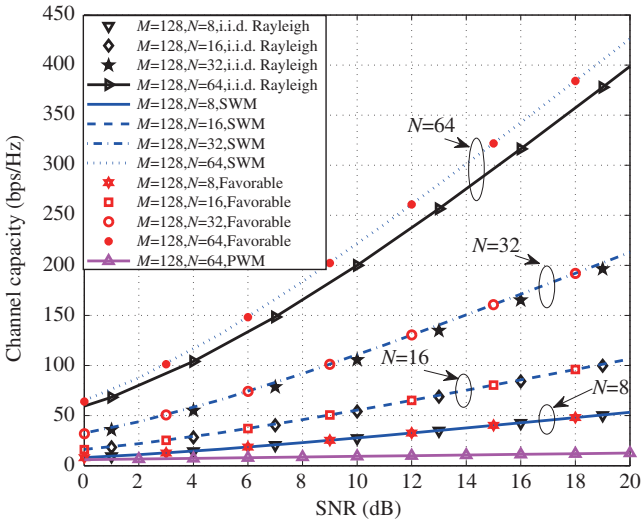

Figure 7 Spherical wave model simulated channel capacity vs. SNR for various conditions.

128 antenna elements. It is obvious that eigenvalue distributions of different M and K pairs in cells of different sizes change considerably. When $R_c \leqslant R_{\mathrm{FRBLMA}}/40$, the case corresponding to $K = 32$ shows low similarity between the spherical wave model and the plane wave model. This is accordant with the results (large MSE values) in Table 1. Compared with the $K = 8$ case, the likelihood of an eigenvalue of one is decreased. This means that the orthogonality of the row vector decreases when users increase. This is because—as we have noted—very tall or very wide matrices tend to be very well conditioned, and tend to have equal eigenvalues. From results in Figure 8 for the cases of $R_c \leqslant R_{\mathrm{FRBLMA}}/4$ and $R_c \leqslant R_{\mathrm{FRBLMA}}$, this phenomenon also can be observed. When considering larger wireless coverage, i.e., $R_c \leqslant R_{\mathrm{FRBLMA}}/4$ and $R_c \leqslant R_{\mathrm{FRBLMA}}$, distributions of the spherical wave model are in good agreement with distributions of the plane wave model, causing small MSE values which are the same as the values listed in Table 1. This is because when the distance between the user and the base-station increases, the incident angle differences among the user-elements become asymptotically zero. The spherical wave can be very well approximated by the plane wave, and hence the eigenvalues of the two types of models are similar.

Next, the favorable propagation in which the elements of $\boldsymbol{H}$ follow the i.i.d. Rayleigh distribution is considered. The asymptotic eigenvalue distribution of the favorable propagation matrix $\boldsymbol{W}$ follows the Marcenko-Pastur law (see Eqs. (1.10)–(1.12) in [21]). When considering the $K = 8$ case, the eigenvalues of the i.i.d. Rayleigh model vary around the value of one, and are spread less. Whereas, the i.i.d. Rayleigh results of $K = 32$ are more widely distributed than those of $K = 8$. This means the $K = 8$ case shows

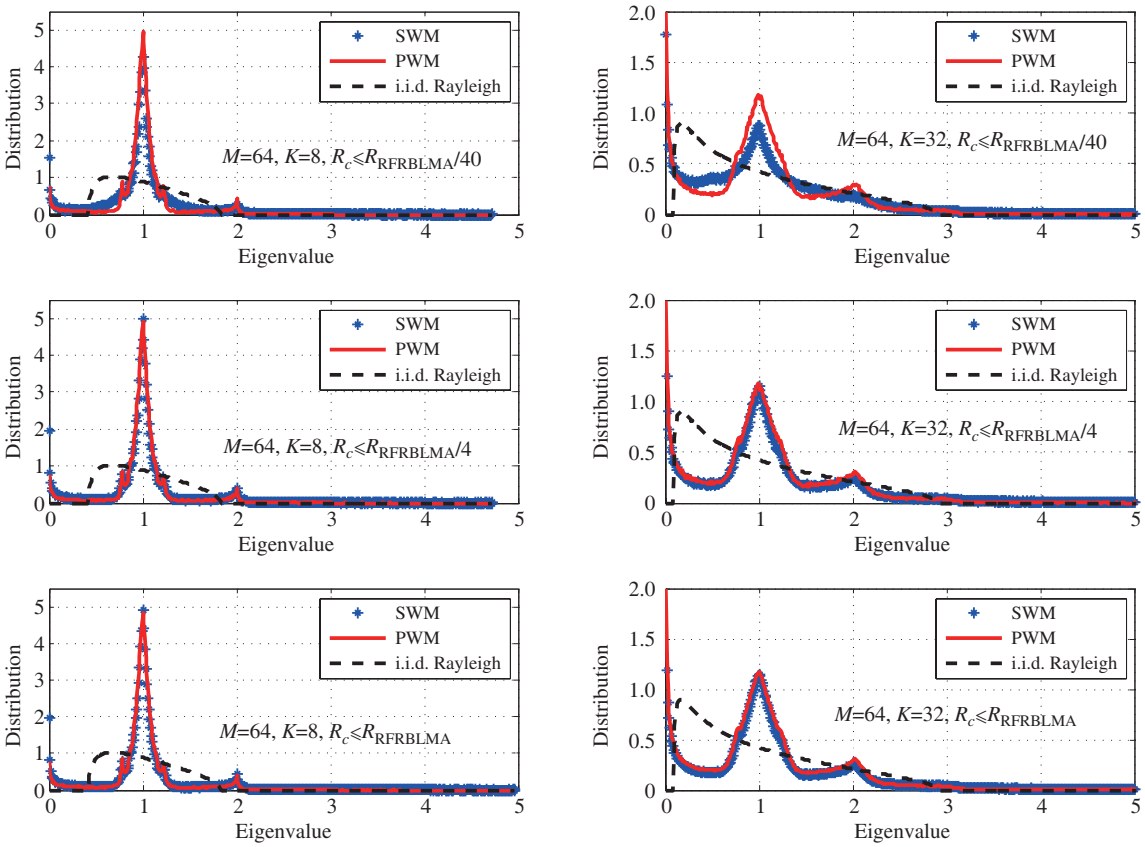

Figure 8 Eigenvalue distributions of simulation cases.

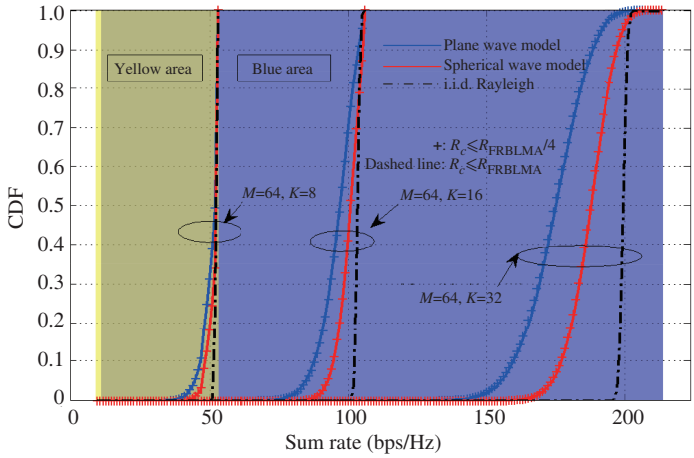

Figure 9 CDF of sum rates of simulation cases.

higher similarity of the favorable propagation condition compared with the $K = 32$ case. This also can be attributed to the matrix changing from the tall or wide shape to the square shape. The difference also can be found in the subsequent simulation result, from the deviation value from the upper boundary of the sum rate.

Figure 9 presents the cumulative distribution function (CDF) of sum rates in different simulation cases. We consider three cases that the base-station serves $K = 8$, $K = 16$ and $K = 32$ users, with the SNR of 20 dB. It is known that the sum-rate is linearly proportional to the number of users K if the pairwise channel vectors are orthogonal. Hence the sum rate changes considerably with the number of users. From this figure, we can see that for different values of K, the deviation value from the i.i.d Rayleigh model

of the PWM is larger than that of the SWM. This is caused by the fact that the incidence/departure angle of each propagation ray differs from each other for the spherical wave propagation, whereas this angle value is approximately the same in the plane wave assumption, causing the decrease of diversity and independent fading. These different angles are more likely to make the inner product of the channel vectors (28) approach zero. As for the CDF difference between the i.i.d. Rayleigh channel and the plane wave model for different K values, the gap increases as the number of users increases. We also consider the same matrix theory explanation previously provided. The increasing "squaring" of the matrix degrades the condition result. Furthermore, in Figure 9 we can see that the "+" line and the dashed line, corresponding to the conditions that users are distributed at the ranges of $R_c \leqslant R_{\mathrm{FRBLMA}}/4$ and $R_c \leqslant R_{\mathrm{FRBLMA}}$ respectively, fit significantly well. We can conclude that when the users are randomly distributed, the sum rates are essentially independent of the cell size.

Finally, we also plot two colored areas in Figure 9, yellow and blue, which represent the sum rate ranges of $K = 8$ and $K = 32$. The upper and lower boundaries of each area are determined by the best and worst propagation conditions: (1) all of the eigenvalues are equal; in other words, the channel vector of each user is perfectly orthogonal to all others; and (2) all but one of the eigenvalues is equal to zero. As for $K = 8$, the sum rate curves, PWM, SWM and i.i.d. Rayleigh, all approach the upper boundary closely, whereas the curves of the blue area $K = 32$ stand far away. This is also attributed to the former matrix condition explanation.

6 Conclusion

The linear massive MIMO system having a large number of antenna elements is likely to be an emerging system that can significantly improve the frequency and power efficiency of future wireless systems. We have used a spherical wave model (SWM) to characterize both the peer to peer (PTP) and multi-user (MU) linear massive MIMO systems. For the PTP system, a geometrical optimization method is proposed to make the channel matrix achieve the full rank value. This method specifies some values for transmitter and receiver distance, the element separation and the rotation angle of the antenna array, by which full spatial diversity can be obtained even in LOS scenarios. In MU systems, the simulation results show that the eigenvalue distribution of the channel matrix obtained from the PWM spreads more than the value from the SWM, and more realistic SWM characterized system can achieve a higher sum rate than the PWM in LOS propagation scenarios. Our findings reveal that the SWM method is necessary in the massive MIMO channel characterization, since its properties differ considerably from the channel properties of the PWM. This provides the basis for the practical deployment of massive MIMO wireless networks. Furthermore, the massive MIMO system can be configured with different shapes of antenna arrays, e.g., linear, circular, squared or cylindrical. Additional investigation into different shapes of antenna arrays from a spherical wave model perspective is planned for future work.

Acknowledgements

This work was supported in part by National High-tech R&D Program of China (863 Program) (Grant No. 2014AA01A706), Fundamental Research Funds for the Central Universities (Grant No. 2014JBZ001), National Natural Science Foundation of China (Grant No. 61471027), Beijing Nova Programme (Grant No. xx2016023), Research Fund of National Mobile Communications Research Laboratory, Southeast University (Grant No. 2014D05), and Beijing Natural Science Foundation Project (Grant No. 4152043). We would like to thank the anonymous referees for their help in improving this paper.

Conflict of interest The authors declare that they have no conflict of interest.

References

1 Rusek F, Persson D, Lau B K, et al. Scaling up MIMO: opportunities and challenges with very large arrays. IEEE Signal Process Mag, 2013, 30: 40–60

2 Larsson E, Edfors O, Tufvesson F, et al. Massive MIMO for next generation wireless systems. IEEE Commun Mag, 2014, 52: 186–195
3 Ngo H Q, Larsson E, Marzetta T. Energy and spectral efficiency of very large multiuser MIMO Systems. IEEE Trans Commun, 2013, 61: 1436–1449
4 Ma Z, Zhang Z Q, Ding Z G, et al. Key techniques for 5G wireless communications: network architecture, physical layer, and MAC layer perspectives. Sci China Inf Sci, 2015, 57: 041301
5 Wu S, Wang C X, Haas H, et al. A non-stationary wideband channel model for massive MIMO communication systems. IEEE Trans Wirel Commun, 2015, 14: 1434–1446
6 Wu S, Wang C X, Aggoune E-H, et al. A non-stationary 3-D wideband twin-cluster model for 5G massive MIMO channels. IEEE J Sel Area Commun, 2014, 32: 1207–1218
7 Ngo H Q, Larsson E, Marzetta T. Aspects of favorable propagation in massive MIMO. In: Proceedings of the 22nd European Signal Processing Conference (EUSIPCO), Bristol, 2014. 76–80
8 Xing C W, Ma S D, Fei Z S, et al. A general robust linear transceiver design for multi-hop amplify-and-forward MIMO relaying systems. IEEE Trans Signal Process, 2013, 61: 1196–1209
9 Bohagen F, Orten P, Oien G. Construction and capacity analysis of high-rank line-of-sight MIMO channels. In: Proceedings of IEEE Wireless Communications and Networking Conference (WCNC), New Orleans, 2005. 432–437
10 Bohagen F, Orten P, Oien G. Design of optimal high-rank line-of-sight MIMO channels. IEEE Trans Wirel Commun, 2007, 6: 1420–1425
11 Bohagen F, Orten P, Oien G. On spherical vs. plane wave modeling of line-of-sight MIMO channels. IEEE Trans Commun, 2009, 57: 841–849
12 Popovski P, Braun V, Ren Z. Deliverable D1.1 Scenarios, requirements and KPIs for 5G mobile and wireless system. Mobile and wireless communications Enablers for the Twenty-twenty Information Society. Technical Report. 2013
13 Rappaport T, Sun S, Mayzus R, et al. Millimeter wave mobile communications for 5g cellular: It will work! IEEE Access, 2013, 1: 335–349
14 Hoydis J, Hosseini K, Brink S T, et al. Making smart use of excess antennas: massive MIMO, small cells, and TDD. BELL Labs Tech J, 2013, 18: 5–21
15 Rade L, Westergren B. Mathematics Handbook for Science and Engineering. Berlin/New York: Springer Lund (Sweden), 2004
16 Haustein T, Kruger U. Smart geometrical antenna design exploiting the los component to enhance a MIMO system based on rayleigh-fading in indoor scenarios. In: Proceedings of the IEEE 14th International Symposium on Personal, Indoor and Mobile Radio Communications, Beijing, 2003. 1144–1148
17 Tse D, Viswanath P. Fundamentals of Wireless Communication. New York: Cambridge University Press, 2005
18 Capps C. Near field or far field? EDN, 2001: 95–101
19 Liu L, Matolak D W, Tao C, et al. Far region boundary definition of linear massive MIMO antenna arrays. In: Proceedings of the 82nd IEEE Vehicular Technology Conference (VTC2015-Fall), Boston, 2015. 1–6
20 Chen S Z, Zhao J. The requirements, challenges, and technologies for 5G of terrestrial mobile telecommunication. IEEE Commun Mag, 2014, 52: 36–43
21 Tulino A M, Verdú S. Random matrix theory and wireless communications. Found Trends Commun Inf Theory, 2004, 1: 1–182. http://dx.doi.org/10.1561/0100000001

Appendix A

Eq. (16) gives the orthogonality requirement that the matrix becomes a diagonal form, or the subchannel is orthogonal. For this reason, we can do some practical approximations to achieve the orthogonality.

The path length term $r_{n,m}^{\mathrm{PS}}$ in (12) can be approximated by using the Binomial Theorem $(1+\Delta)^{1/2} \approx 1+\Delta/2$ when $\Delta \ll 1$. In other words, only the first two terms are maintained. Then the path difference term is approximated as

$$r_{n,m}^{\mathrm{PS}} \approx \left(\left(d+(n-1)\,d_r\cos\varphi\right)-(m-1)\,d_t\cos\theta\right)+\frac{1}{2d}\left((n-1)\,d_r\sin\varphi-(m-1)\,d_t\sin\theta\right)^2. \tag{A1}$$

Here we assume that the distance between two antenna arrays is much larger than the project values of the antenna arrays on the x axis. The second simplification is performed in the denominator of the fraction term in (A1). The path difference that nth element and mth element projected on x axis is removed. This is valid when d is larger than the array lengths in the x direction. Subsequently, (15) can be simplified as

$$\begin{aligned}\left(\boldsymbol{W}_{N\times N}^{\mathrm{PS}}\right)_{n_1,n_2} &= \sum_{m=1}^{M}\exp\left(\mathrm{j}\frac{2\pi}{\lambda}\left(r_{n_1,m}^{\mathrm{PS}}-r_{n_2,m}^{\mathrm{PS}}\right)\right)\\ &= \sum_{m=1}^{M}\exp\left(\mathrm{j}\frac{2\pi}{\lambda d}\left(m-1\right)d_t d_r\sin\theta\sin\varphi\left(n_2-n_1\right)\right) \qquad \text{(A2)}\\ &= \frac{\sin(\frac{\pi}{\lambda d}d_t d_r\sin\theta\sin\varphi(n_2-n_1)M)}{\sin(\frac{\pi}{\lambda d}d_t d_r\sin\theta\sin\varphi(n_2-n_1))} \overset{n_1\neq n_2}{=} 0. \qquad \text{(A3)}\end{aligned}$$

In (A2), the phase shift term irrelevant to the amplitude value of $(\boldsymbol{W}_{N\times N}^{\mathrm{PS}})_{n_1,n_2}$ is neglected in the final expression form of (A3). The similar operation will be conducted hereinafter. On one hand, if one of the transmitter array or the receiver array is parallel to the x axis, according to (A3), we can obtain $(\boldsymbol{W}_{N\times N}^{\mathrm{PS}})_{n_1,n_2} = M$. That means that the $\mathrm{rank}(\boldsymbol{W}_{N\times N}^{\mathrm{PS}}) = 1$. On the other hand, if the orientation angle $\theta \neq 0$ and $\varphi \neq 0$, when $M \leqslant N$, the above result can be changed as a similar expression form as

$$\left(\boldsymbol{W}_{M\times M}^{\mathrm{PS}}\right)_{m_1,m_2} = \frac{\sin(\frac{\pi}{\lambda d} d_t d_r \sin\theta \sin\varphi(m_2 - m_1)N)}{\sin(\frac{\pi}{\lambda d} d_t d_r \sin\theta \sin\varphi(m_2 - m_1))}. \tag{A4}$$

Then by using the predefined values U and V, a general element form of (A4) can be expressed as

$$\left(\boldsymbol{W}_{U\times U}^{\mathrm{PS}}\right)_{u_1,u_2} = \frac{\sin(\frac{\pi}{\lambda d} d_t d_r \sin\theta \sin\varphi(u_2 - u_1)V)}{\sin(\frac{\pi}{\lambda d} d_t d_r \sin\theta \sin\varphi(u_2 - u_1))} \overset{u_1\neq u_2}{=} 0. \tag{A5}$$

The general solution of (A5) can be easily obtained as

$$\frac{d_t d_r \sin\theta \sin\varphi V}{\lambda d} = Z, \tag{A6}$$

where Z is a positive nonzero integer and $Z \neq 0$. As for the backhaul system, the distance d, the working frequency with the wavelength of λ, the numbers of the transmitter and receiver antenna elements and the orientation angles of antennas can be pre-defined. In [16] and Gesbert et al.'s work[1)] it is suggested using the parallel antenna arrays ($\theta = \varphi = \pi/2$) can bring benefits. Based on the spherical wave principle, it is intuitive that antenna elements of the parallel antennas will experience a diverse and large angle shift which give rises to the high rank value of the channel matrix. Hence, the antenna arrays are in parallel. In addition, for a practical application, d_t usually equals to d_r and we denote as $d_t = d_r = d_a$. Then according to (A6), we can obtain the first orthogonality requirement as

$$d = d_a^2 V / Z\lambda. \tag{A7}$$

Recalling the Binomial Theorem condition $\Delta \ll 1$, the second requirement is

$$d \gg (n-1)\, d_r \sin\varphi - (m-1)\, d_t \sin\theta. \tag{A8}$$

By using the previous predefined conditions, and due to the facts that $m = 1, 2, \ldots, V$, $n = 1, 2, \ldots, U$, and (A8) can be written as

$$d \gg \max\{|m-n|\}\, d_a = (V-1)\, d_a \quad \rightarrow \quad d > 10\,(V-1)\, d_a. \tag{A9}$$

Substituting (A7) in to (A9), we can obtain the second general orthogonality conditioning as

$$d_a > Z \frac{10\,(V-1)\,\lambda}{V}. \tag{A10}$$

From (A10) we can see that several solutions exist. Here we use the solution $Z = 1$ for the smallest array span reason, and so the final orthogonality conditioning is

$$d_a > \frac{10\,(V-1)\,\lambda}{V} \xrightarrow{V\to\infty} d_a > 10\lambda. \tag{A11}$$

1) Gesbert D, Bolcskei H, Gore D, et al. Outdoor MIMO wireless channels: models and performance prediction. IEEE Trans Commun, 2002, 50: 1926–1934.